Characteristics of Laser-Induced Plasma as a Spectroscopic Light Emission Source

Q.L. Ma[a], V. Motto-Ros[a], W.Q. Lei[a,b], X.C. Wang[a], M. Boueri[a], F. Laye[a], C.Q. Zeng[a], M. Sausy[a], A. Wartelle[a], X.S. Bai[b], L.J. Zheng[b], H.P. Zeng[b], M. Baudelet[c], and J. Yu[a]

[a]*Université de Lyon, F-69622, Lyon, Université Lyon 1, Villeurbanne, CNRS, UMR5579, LASIM, France*
[b]*State Key Laboratory of Precision Spectroscopy, East China Normal University, Shanghai, P. R. China*
[c]*Townes Laser Institute, CREOL-The College of Optics and Photonics, University of Central Florida, Orlando, FL 32816, USA*

Abstract. Laser-induced plasma is today a widespread spectroscopic emission source. It can be easily generated using compact and reliable nanosecond pulsed lasers and finds applications in various domains with laser-induced breakdown spectroscopy (LIBS). It is however such a particular medium which is intrinsically a transient and non-point light emitting source. Its time- and space-resolved diagnostics is therefore crucial for its optimized use. In this paper, we review our works on the investigation of the morphology and the evolution of the plasma. Different time scales relevant for the description of the plasma's kinetics and dynamics are covered by suitable techniques. Our results show detailed evolution and transformation of the plasma with high temporal and spatial resolutions. The effects of the laser parameters as well as the background gas are particularly studied.

Keywords: Laser-induced plasma, Plasma diagnostics, Plasma emission, Plasma morphology, LIBS.
PACS: 52.25.Kn, 52.25.Os, 52.38.Mf, 52.50.Jm, 52.70.Kz

INTRODUCTION

Laser-induced plasma (LIP) represents a frequently used spectroscopic light emission source. It provides particularly the basis of laser-induced breakdown spectroscopy (LIBS), an elemental analytical technique which is currently developed for applications in a wide range of domains [1]. Among them, one can mention the detection of toxic metallic elements in fresh vegetables [2], the classification and identification of bacteria [3], the automated sorting of plastic wastes [4] or the surface elemental analysis/mapping of geomaterials [5]. The use of LIP as a spectroscopic source is however not a recently emerged ideas since a pioneer work has been reported in 1963, three years after the invention of the laser [6]. Only recent investigations showed the necessity of considering LIP as a transient and non-point emission source to improve the performance of the applications [7,8]. Time- and space-resolved diagnostics of the plasma is thus of fundamental importance for LIBS. In this paper, we review our works on the investigation of the morphology and the evolution of the plasma. Suitable techniques have been used to cover different time scales relevant for

the description of the plasma's kinetics and dynamics. Detailed evolution and transformation of the plasma have been observed with high temporal and spatial resolutions. Particular attention has been paid to the effects of the laser parameters as well as the background gas.

BASIC PHYSICAL PROCESSES INVOLVED IN THE EXPANSION OF LASER-INDUCED PLASMA

Optical emission from LIP takes place during its expansion into the background gas. Since the ignition of material breakdown and the initiation of the plasma are much faster than the duration of nanosecond laser pulses typically used for ablation, the early stage of the plasma expansion is driven by laser-supported absorption waves (LSAW) [9]. The absorption of the tailing part of the laser pulse by the interacting system including the ablation vapor from the target and the surrounding background gas compressed and heated by the vapor, is the key point which determines the morphology and the subsequent evolution of the plasma. Laser radiation is absorbed preliminary by inverse bremsstrahlung which dominates as soon as the medium becomes ionized. Its efficiency sensitively increases with the laser wavelength (typically $\sim \lambda^3$). Infrared radiation is thus much more strongly coupled to the plasma which during its evolution includes the ablation vapor as well as the ionized background gas. For UV radiation, photoinization can be efficient for excited states of easily ionized elements, metallic vapor for example. The absorption of laser radiation by the plasma accelerates its propagation towards the laser coming direction and leads to its anisotropic expansion.

In typical laser-induced plasmas, the relation between the atomic state distribution function and the plasma parameters is described by the local thermodynamic equilibrium (LTE) [10]. In such a state, the balances of Boltzmann, Saha and Maxwell types hold, while that of Planck fails. The unique temperature which characterizes the distribution laws of the three balanced processes allows the quantitative determination of the concentrations of different elements contained in the plasma according to the procedure of calibration-free LIBS [11]. The check and validation of LTE in laser-induced plasma often needs several independent approaches [12]. A necessary condition is provided by the McWhirter criterion which determines the minimal value of electron density allowing the domination of collisional excitations of atoms and ions by electrons over the radiation process. Further validation with the excitation temperatures of the different species in the plasma provides the sufficient condition for LTE if all these temperatures tend to a unique value.

TECHNIQUES FOR TIME- AND SPACE-RESOLVED PLASMA DIAGNOSTICS

In our investigations, several time- and space-resolved techniques have been used to cover different time scales suitable to describe the evolution of the plasma. Figure 1 summarizes these time scales together with the corresponding diagnostics techniques used in our experiments.

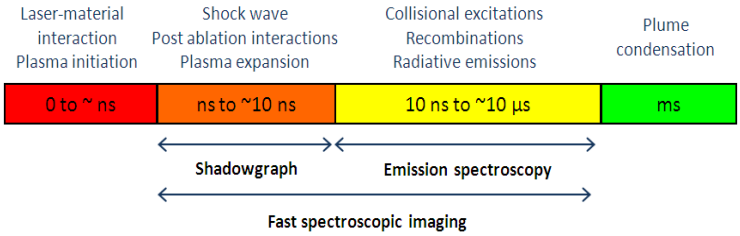

FIGURE 1. Characteristic time scales after the laser impact and the associated diagnostics techniques.

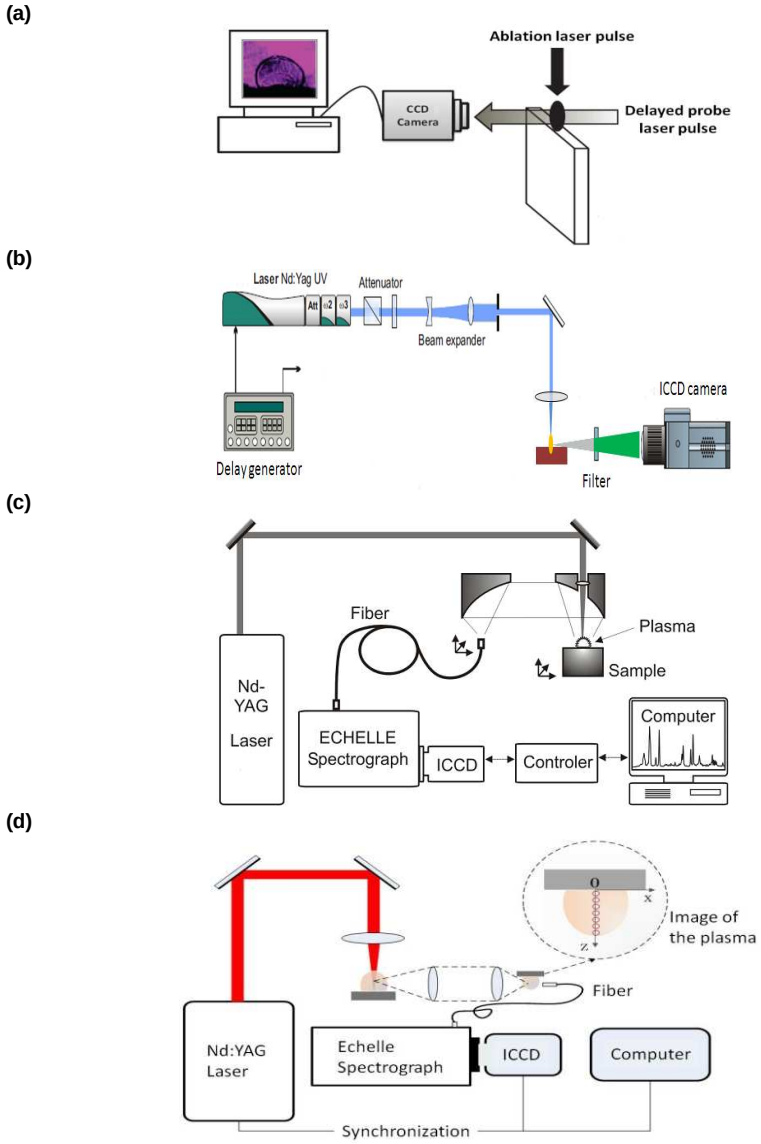

FIGURE 2. Schematics of used experimental setups. See the text for the details.

Figure 2 schematically illustrates the plasma diagnostics techniques used in our studies. Figure 2(a) shows the setup of time-resolved shadowgraph where a delayed probe pulse passes through the plasma. Its shadow due to the inhomogeneity induced by the shockwave is directly recorded by a CCD camera. The use of a femtosecond

laser pulse synchronized with the ablation pulse allows ps-range time resolution. Figure 2(b) illustrates the setup of fast spectroscopic imaging where the plasma is directly imaged by an ICCD camera with a time resolution up to 2 ns. Specific species can be selected using narrow band spectral filters centered on the emission lines of the species. In Figures 2(c) and 2(d), the setups of emission spectroscopy are shown. The difference is in (c), only the time resolution is available thanks to the use of an ICCD camera coupled to an Echelle spectrograph, the plasma emission is space-integrated by a pair of parabolic mirrors. Full time- and space-resolutions are available in Figure 2(d) where a fiber with a 50-µm diameter core is placed on the imaging plane of the plasma to locally probe the emission from the plasma. The further detailed descriptions of these setups can be found elsewhere in our published papers.

RESULTS ON TIME- AND SPACE-RESOLVED PLASMA DIAGNOSTICS

The early stage propagation of the plasma is characterized by shockwave expansion as shown in Figure 3. We can see different behaviors for UV (226 nm) and IR (1064 nm) ablations [13]. For UV ablation, the shockwaves remain spherical, while those for IR ablation exhibit strong anisotropy with an elongated form. This clearly shows the effect of LSAW for IR ablation. Significant laser energy is absorbed in the vicinity of the shockwave front by either the compressed and heated background gas or ablation vapor under the shock front. This results in the accelerated propagation of the plasma along the laser incident axis.

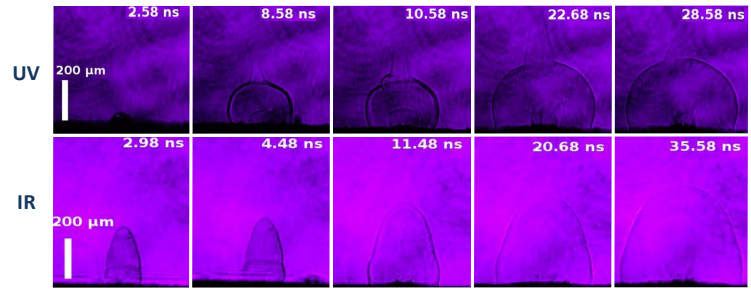

FIGURE 3. Time-resolved shadowgraphs for UV(266 nm) and IR (1064 nm) ablations at an irradiance of 15 GW/cm^2.

Figures 4 shows fast spectroscopic images obtained for IR ablation of an aluminum target in argon ambient. The confinement of the Al vapor by Ar is clearly observed. Such confinement has two benefic effects for a stable emission from the plasma: i) spatially delimiting the extension of the emission source in a region of ~ 1 mm in diameter; ii) thermally confining the plasma for a longer radiative lifetime.

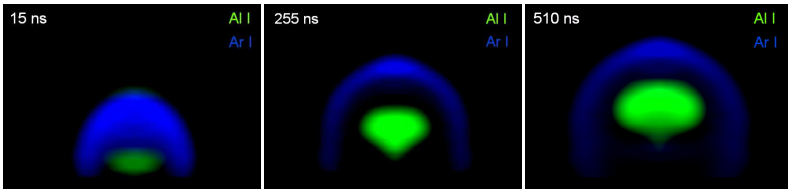

FIGURE 4. Fast spectroscopic images of the plasma consisting of an Al ablation vapor propagating into Ar background.

The validation of the LTE state is shown in Figure 5 for plasma from a plastic sample (PP) ablated with UV pulses. The measurement of the electron density shows that the McWhirter criterion is satisfied for a delay < 2 µs, which provides the necessary condition for LTE. The further determination of temperatures of different species in the plasma shows that they merge into a single value for a delay > 800 ns. The plasma is therefore in LTE for delays larger than 800 ns and smaller than 2 µs [7].

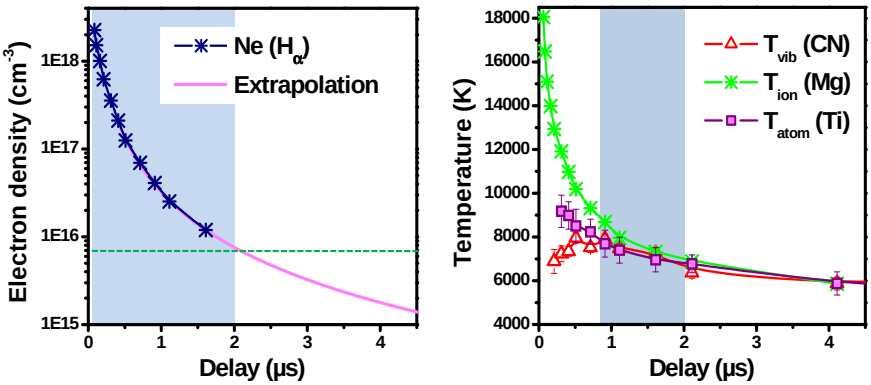

FIGURE 5. Validation of LTE with the necessary and sufficient conditions.

Over the period where the plasma approaches LTE, we determine the axial profiles of the electron density and the temperature using time- and space-resolved emission spectroscopy for both UV and IR ablations. The results (Figure 6) show that for UV ablation, the plasma has a higher electron density and a higher temperature, while for IR one, the plasma has a larger axial extent with a lower electron density and temperature. However the plasma is much more homogenous for IR ablation [8]. These observations are consistent with the above presented shadowgraphs and correspond to the different absorption behaviors of the plasma for UV and IR radiations.

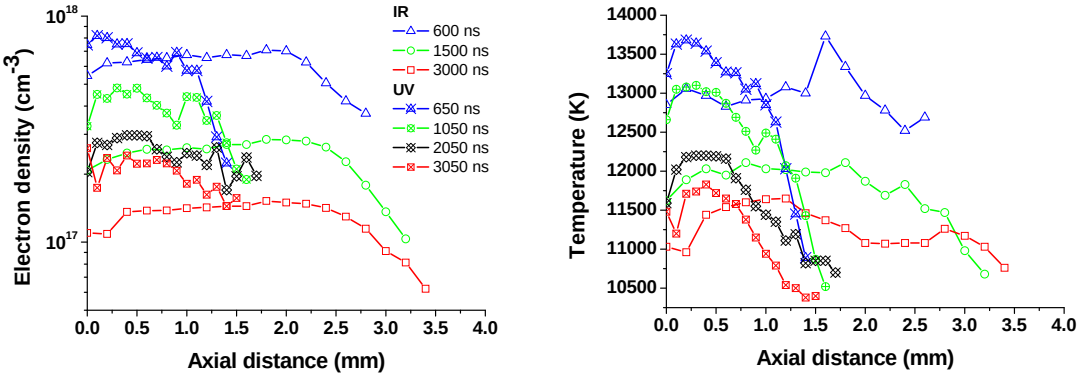

FIGURE 6. Axial profiles of electron density and temperature for UV and IR ablations at different delays (600 to 3000 ns).

Finally in Figure 7, we show the stability of the emission obtained with a gated and localized detection which takes into account the time- and space-evolutions of the plasma (UV ablation of a glass sample). The shot-to-shot repeatability of the Al I 394 nm line is 5.6% (RSD). This result is significantly improved by normalizing the intensity with that from an internal reference (Si) to reduce the effect of the fluctuation of laser energy. We get a repeatability of 3.5% (RSD) for the normalized intensity.

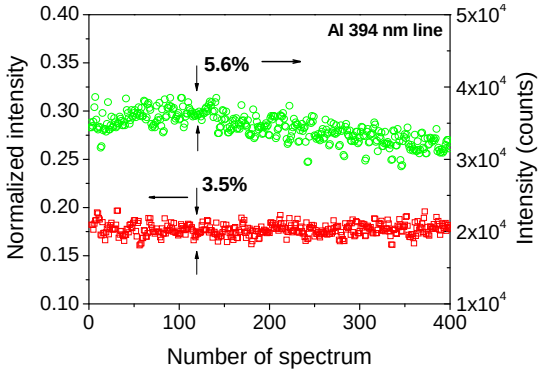

FIGURE 7. Shot-to-shot repeatability of the plasma emission over 400 individual spectra.

CONCLUSION

We have reviewed in this paper our investigations on the characteristics of laser-induced plasma as a spectroscopic light emission source. Especially, the morphology and the evolution of the plasma have been shown together with the effects of the laser parameters and the background gas. Our results allow us to conclude that gated and localized detection optimizes the use of such a transient and expanding light emission source, and that an emission repeatability of 3.5% can be typically obtained.

ACKNOWLEDGMENTS

The authors thank the French Rhone-Alps Region for their supports through the CMIRA international collaboration program.

REFERENCES

1. A. W. Miziolek, V. Palleschi, I. Schechter, *Laser-induced breakdown spectroscopy: Fundamental and applications*, Cambridge University Press, 2006.
2. V. Juvé, R. Portelli, M. Boueri, M. Baudelet, et al., *Spectrochim. Acta Part B* **63**, 1047–1053 (2008).
3. M. Baudelet, J. Yu, M. Bossu, J. Jovelet, J.P. Wolf, T. Amodeo, E. Fréjafon, P. Laloi, *Appl. Phys. Letters* **89**, 163903 (2006).
4. M. Boueri, V. Motto-Ros, W. Q. Lei, Q. L. Ma, L. J. Zheng, H. P. Zeng and J. Yu, Appl. Spectroscopy **65**, 307-314 (2011).
5. Q. L. Ma, V. Motto-Ros, W. Q. Lei, M. Boueri, L. J. Zheng, H. P. Zeng, M. Bar-Matthews, A. Ayalon, G. Panczer, and J. Yu, *Spectrochim. Acta Part B* **65**, 707-714 (2010).
6. J. Debras-Guédon, N. Liodec, *C.R. Acad. Sci.* **257**, 3336-3339 (1963).
7. W. Q. Lei, V. Motto-Ros, M. Boueri, Q. L. Ma, D. C. Zhang, L. J. Zheng, H. P. Zeng, and J. Yu, *Spectrochim. Acta Part B* **64**, 891-898 (2009).
8. Q. L. Ma, V. Motto-Ros, W. Q. Lei, M. Boueri, X. S. Bai, L. J. Zheng, H. P. Zeng, and J. Yu, *Spectrochim. Acta Part B* **65**, 896-907 (2010).
9. R. G. Root, "Modeling of Post-Breakdown Phenomena" in *Laser-Induced Plasmas and Applications*, edited by L. J. Radziemski and D. A. Cremers, New York: Dekker, 1989, 69-103.
10. J. A. M. Van Der Mullen, *Spectrochim. Acta Part B* **45**, 1–13 (1990).
11. A. Ciucci, M. Corsi, V. Palleschi, S. Rastelli, A. Salvetti, and E. Tognoni, *Applied Spectroscopy*, **53**, 960-964 (1999).
12. D. W. Hahn and N. Omenetto, *Applied Spectroscopy*, **64**, 335A-366A (2010).
13. M. Boueri, M. Baudelet, J. Yu, X.L. Mao, S. S. Mao, and R. Russo, *Appl. Surf. Sci.* **255**, 9566-9571 (2009).